



# Vibrational behavior of multi-layer plates in broad-band frequency range: comparisons between experimental and theoretical estimations

Kerem Ege, Valentin Henry, Q. Leclerc, R.G. Rinaldi, Céline Sandier

## ► To cite this version:

Kerem Ege, Valentin Henry, Q. Leclerc, R.G. Rinaldi, Céline Sandier. Vibrational behavior of multi-layer plates in broad-band frequency range: comparisons between experimental and theoretical estimations. InterNoise 2015, Aug 2015, San Francisco, United States. pp.218. hal-01215310

**HAL Id: hal-01215310**

**<https://hal.science/hal-01215310>**

Submitted on 30 Apr 2018

**HAL** is a multi-disciplinary open access archive for the deposit and dissemination of scientific research documents, whether they are published or not. The documents may come from teaching and research institutions in France or abroad, or from public or private research centers.

L'archive ouverte pluridisciplinaire **HAL**, est destinée au dépôt et à la diffusion de documents scientifiques de niveau recherche, publiés ou non, émanant des établissements d'enseignement et de recherche français ou étrangers, des laboratoires publics ou privés.



## **Vibrational behavior of multi-layer plates in broad-band frequency range: comparisons between experimental and theoretical estimations**

Kerem Ege<sup>a)</sup>

Valentin Henry<sup>b)</sup>

Quentin Leclère<sup>c)</sup>

Laboratoire Vibrations Acoustique, INSA-Lyon, 25 bis Avenue Jean Capelle,  
F-69621 Villeurbanne Cedex, France

Renaud G. Rinaldi<sup>d)</sup>

MATEIS CNRS UMR5510, INSA-Lyon, 7 Avenue Jean Capelle  
F-69621 Villeurbanne Cedex, France

Céline Sandier<sup>e)</sup>

Laboratoire Vibrations Acoustique, INSA-Lyon, 25 bis Avenue Jean Capelle,  
F-69621 Villeurbanne Cedex, France

**In the context of aeronautics, automotive and construction applications the design of lightened multilayer plates with optimized vibroacoustical damping and isolation performances remains a major industrial challenge and a hot topic of research. This paper focuses on the vibrational behavior of three-layer composites plates in broad-band frequency range. Several aspects are studied through measurement techniques and analytical modeling of two sandwich systems: symmetrical steel/polymer/steel and nonsymmetrical steel/polymer/aluminum plates. Contactless measurements of the velocity field made using a scanning laser vibrometer allow estimating the equivalent single layer complex rigidity in the mid/high frequency ranges. Coupled with low/mid frequency estimations obtained with a high-resolution modal analysis method, the frequency dependent equivalent Young's modulus and equivalent loss factors of the two composites plates are finally identified for the whole [0-5 kHz] band. The results are in very good agreement with an equivalent single layer analytical modeling based on wave propagation analysis. The comparison with this model allows identifying the frequency dependent complex modulus of the polymer core layer through inverse resolution. Dynamical mechanical analysis measurements are also performed on the polymer layer alone to compare with the values obtained through inverse method. Again, a good agreement**

---

<sup>a)</sup> email: kerem.ege@insa-lyon.fr

<sup>b)</sup> email: valentin.henry@insa-lyon.fr

<sup>c)</sup> email: quentin.leclere@insa-lyon.fr

<sup>d)</sup> email: renaud.rinaldi@insa-lyon.fr

<sup>e)</sup> email: celine.sandier@insa-lyon.fr

between these two estimations over the broad-band frequency range demonstrates the validity of the approach.

## 1 INTRODUCTION

The present paper is concerned with the study of the vibrational behavior of multilayer stiff lightweight plates in broad-band frequency range. By reducing weight while keeping high stiffness performances, sandwich systems are increasingly used by today's transport and construction industries for example. In this context, the design of lightened multilayer plates with optimized damping and isolation performances, for given frequency bands, remains a major industrial challenge and a hot topic of research. In this article we present and compare experimental and analytical vibroacoustics methods identifying the frequency dependent equivalent Young's modulus and equivalent loss factors of different three-layer plates up to the high-frequency domain.

In a first part, the plates under study are presented and the experimental protocols of the different vibratory measurements are detailed. Using traditional modal analysis in the low frequency domain and finite-element model (FEM) calculations, the equivalent Young's modulus is identified up to 800 Hz. Then, a high-resolution modal analysis method allows identifying equivalent loss factor up to 2.5-3 kHz where modal overlap is high. To conclude this part, contactless measurements of the velocity field (CFAT approach) extend the identification of the complex Young's modulus up to 5 kHz and confirm both previous modal analyses estimations.

Results are compared in section 3 with the predictions obtained using an equivalent single layer analytical modeling based on wave propagation analysis. Finally, the article ends with the identification of the complex modulus of the polymer (core) and its comparison with DMA measurements/extrapolations.

## 2 EXPERIMENTAL PROTOCOL – VIBRATORY MEASUREMENTS

### 2.1 Three-layer plates

The sandwich plates under study are constituted of three homogeneous layers: two metal face sheets and a polymer core (see Figure 1). Two sets of hybrid composites are studied: symmetrical steel/polymer/steel and nonsymmetrical steel/polymer/aluminum rectangular plates of overall dimensions of 300 x 400 x 1 mm<sup>3</sup>. The nature of the polymer core and the thicknesses of the constitutive layers are confidential.

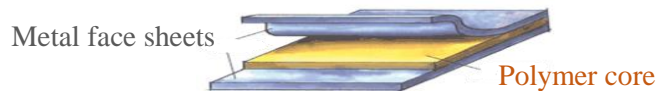


*Fig. 1 –Schematic view of the constitutive parts of a typical three-layer sandwich plate under study*

Although different plates have been measured for each sandwich systems, this paper will focus on only two representative plates called “SPS” and “SPA” plates for “steel/polymer/steel” and “steel/polymer/aluminum” plates respectively. Typical frequency responses (Acceleration/Force) for these two plates obtained from impact hammer excitation (see next section for the experimental protocol) are presented in Figure 2. The low frequency domain is characterized by distinct resonance peaks and the strong modal character of the vibratory behavior (here up to around 700-800 Hz). The modal analysis and the identification of the Young's modulus in low frequency domain will be presented in section 2.2 for the SPS plate.

When the frequency increases, the traditional modal identification methods cannot be used anymore: damping increases, resonances are thus less pronounced, modes overlap and the frequency-response tends to a smooth curve. ESPRIT<sup>1,2</sup> algorithm will be used to identify modal loss factor for this frequency domain on both SPS and SPA plates in section 2.3. Finally in the high-frequency domain (here above 2.5-3 kHz), the vibration can be described as a diffuse wavefield and modal approaches are unsuitable. Thus, the estimation of the complex Young's modulus for both plates and for wide frequency band will be achieved using CFAT methodology in section 2.4.

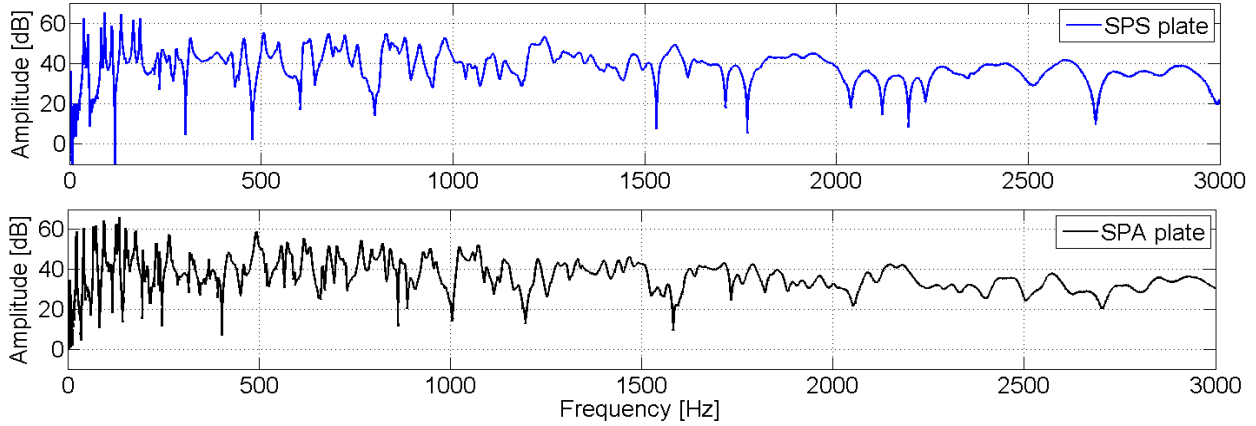


Fig. 2 –Typical frequency responses “Acceleration/Force” (Fourier spectrum) for the SPS plate (top) and the SPA plate (bottom).

## 2.2 Modal analysis in the low frequency domain and equivalent Young's modulus identification

To begin, a modal analysis of the SPS plate is performed in order to estimate the first modal frequencies, loss factors and modal shapes. A pseudo-impulse force is applied by means of a small impact hammer (*P.C.B. Piezotronics 086E80*) on a regular rectangular mesh of 99 points. Boundary conditions are kept as close as possible to “free-free”, by suspending the plate from one of its corner (with rubber bands passing through a tiny hole). The acceleration is measured with a lightweight accelerometer (*P.C.B. Piezotronics M353B18*) fixed on another corner of the plate. Under the chosen boundary conditions, this location is not on any of the nodal lines. A multi-degree-of-freedom curve fitting method (*Rational Fraction Polynomial-Z*) is used to estimate modal frequencies, loss factors and modal shapes.

In parallel with the experimental modal analysis, a finite-element model (FEM) calculation of the normal modes of the same “free-free” SPS plate has been conducted through *MSC NASTRAN* software. Four-noded isoparametric flat plate elements of 1 mm size each have been chosen. Modal frequency convergence criterion has been used to select this element size ensuring far enough points per wavelength (more than 100) up to 800 Hz.

Examples of experimental and numerical mode shapes comparisons are given in Figure 3, where numerical modal shapes are extracted on the experimental mesh points. The Modal Assurance Criterion<sup>3</sup> (called “MAC”) is used here to compare the two sets of results. This numerical tool calculates to what extent a given modal shape fits another one. More precisely, it consists in calculating the spatial correlation between these two functions as given in Equation (1):

$$\text{MAC}(\phi_{m,n}^{exp}, \phi_{p,q}^{num}) = \frac{(\phi_{m,n}^{expT} \phi_{p,q}^{num})}{(\phi_{m,n}^{expT} \phi_{m,n}^{exp})(\phi_{p,q}^{numT} \phi_{p,q}^{num})} \quad (1)$$

where  $\phi_{m,n}^{exp}$  is the experimental modal shape of the  $(m,n)$  plate mode and  $\phi_{p,q}^{num}$  is the numerical modal shape of the  $(p,q)$  plate mode (extracted on the experimental mesh points).

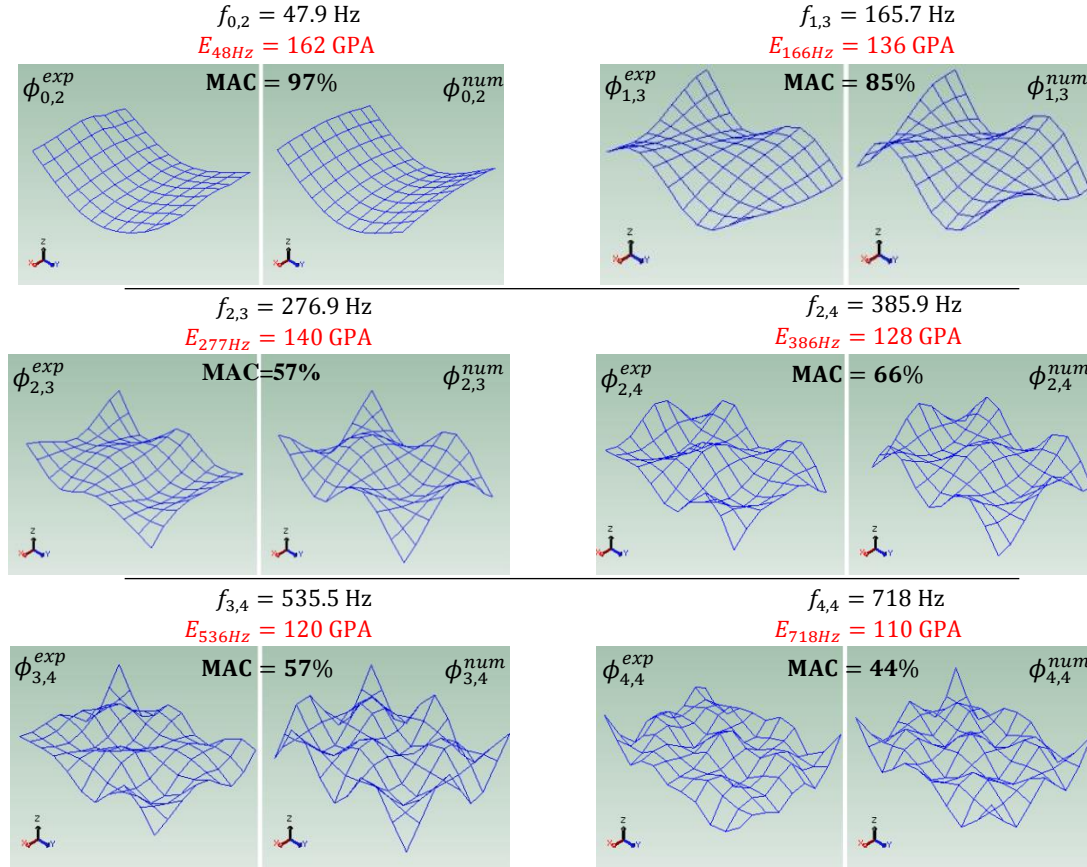


Fig. 3 – Comparisons of six experimental and numerical mode shapes of the Steel/Polymer/Steel plate in the low-frequency domain (numerical mode shapes are extracted on the experimental mesh). For each mode, the MAC value and identified equivalent Young's modulus (by matching FEM estimation to measured modal frequency) are displayed in black bold and red respectively.

As presented in Figure 3, the MAC values are close to 100% for the first low-frequency modes and generally decreases with the modal orders. Indeed, values are directly dependent on the experimental mesh size compared to wavelength. In this study, with 4 cm of distance between two successive excitation points, the modal identification has been successfully done up to 800 Hz, with MAC generally higher than 60%.

Thanks to this experimental/numerical comparison, a first equivalent Young's modulus estimation of the three-layer SPS plate has been conducted as follow: for each identified mode, the numerical Young's modulus is adjusted so that the numerical modal frequency fits the corresponding experimental one, all other parameters remaining constant (dimensions, thickness and density of the equivalent FEM plate are fixed to the measured values; the Poisson's ratio  $\nu$  is arbitrarily set to 0.34). Identified frequency dependent equivalent Young's moduli  $E_{eq}$  are presented in Figure 4 with corresponding MAC values (red for estimations with highest MAC

close to 100%, green for MAC around 70%, and blue for MAC lower than 60%). Equivalent loss factors  $\eta_{eq}$  estimated from the modal analysis are presented in Figure 5 in red. Discussion on these results is done in section 3.2.

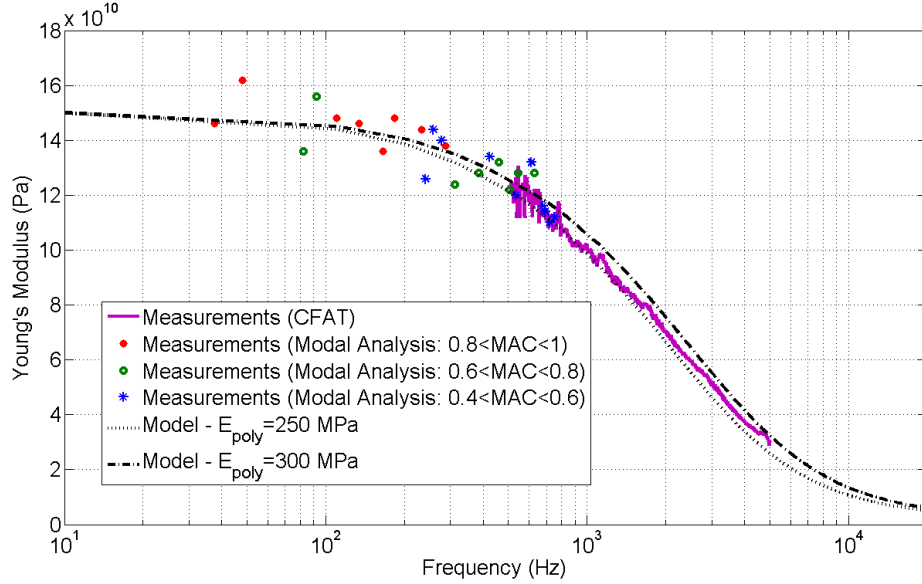


Fig. 4 –Equivalent Young's modulus  $E_{eq}$  – Steel/Polymer/Steel (SPS) plate

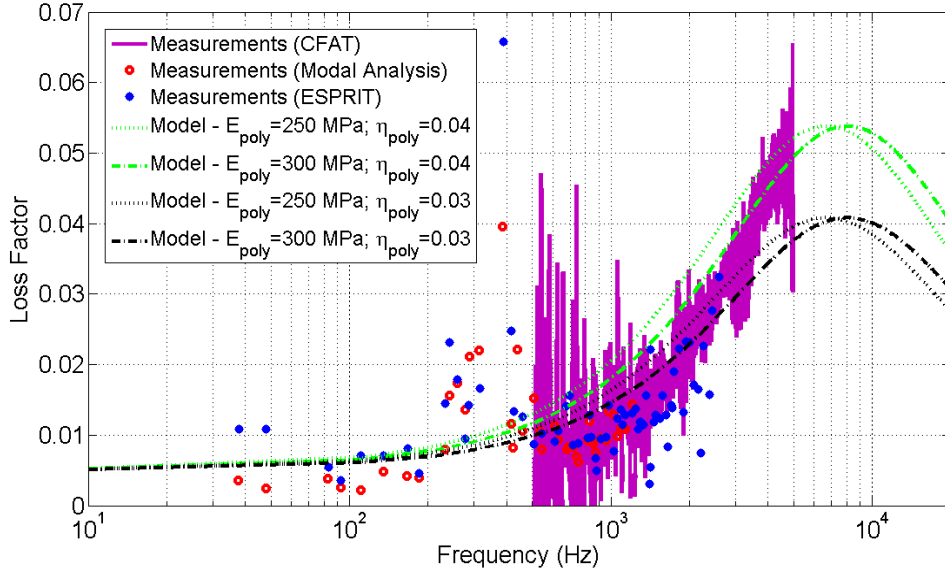


Fig. 5 –Equivalent loss factor  $\eta_{eq}$  – Steel/Polymer/Steel (SPS) plate

### 2.3 Loss factors estimations in the mid-frequency domain – ESPRIT algorithm

In order to identify the equivalent loss factors of the multi-layer plates at higher frequencies, an high-resolution modal analysis technique<sup>1</sup> based on ESPRIT algorithm<sup>2</sup> is used. This high-resolution method assumes that the signal  $s(t)$  is a sum of complex exponentials  $x(t)$  (the modal signal to be determined) and white noise  $\beta(t)$ :

$$s(t) = x(t) + \beta(t) = \sum_{k=1}^K a_k e^{-\alpha_k t} e^{i(2\pi f_k t + \varphi_k)} + \beta(t) = \sum_{k=1}^K b_k z_k^t + \beta(t) \quad (2)$$



where  $K$  is the number of complex exponentials,  $b_k = a_k e^{i\varphi_k}$  are the complex amplitudes (with  $a_k$  and  $\varphi_k$  the modal amplitudes and phases at the point of interest), and  $z_k = e^{-\alpha_k t} e^{i 2\pi f_k t}$  the so-called poles (with  $f_k$  the modal frequencies in Hz and  $\alpha_k$  the modal damping factors in  $s^{-1}$ ). The modal damping factor  $\alpha_k$  (also called modal decay constant in  $s^{-1}$ ), the modal decay time  $\tau_k$  (in s) and the modal loss factor  $\eta_k$  (dimensionless) are related between them as follows:

$$\alpha_k = \frac{1}{\tau_k} = \frac{\eta_k \omega_k}{2}, \quad \eta_k = \frac{\Delta f_{k,-3dB}}{f_k} = \frac{\alpha_k}{\pi f_k} \quad (3)$$

where  $\omega_k$  is the modal angular frequency (in  $\text{rad.s}^{-1}$ ) and  $\Delta f_{k,-3dB}$  the half-power modal bandwidth. The rotational invariance property of the signal subspace (see Roy *et al.*<sup>2</sup> for mathematical developments) is used to estimate the modal parameters: frequencies, damping factors and complex amplitudes. The dimensions of both subspaces must be chosen *a priori* and the quality of the estimation depends significantly on a proper choice for these parameters. The best choice for the dimension of the modal subspace is the number of *complex* exponentials actually present in the signal. This number ( $K$ ) is twice the number of *real* decaying sinusoids (modes). Prior to the modal analysis itself, an estimate of this number is obtained by means of the ESTER (ESTimation ERror) technique<sup>4</sup> which consists in minimizing the error on the rotational invariance property of the signal subspace spanned by the sinusoids. The block diagram in Figure 6 describes the three main steps of the high-resolution method: (a) reconstruction of the acceleration impulse response, (b) signal conditioning (band-pass filtering, downsampling...) as proposed by Laroche<sup>5</sup>, (c) order detection, and (d) determination of modal parameters. More details on the different steps of the method are given in Ege *et al.*<sup>1</sup>, where the method is validated on measured and synthesized signals for frequency domain where the Fourier transform meets its limits (due to high modal overlap or poor signal-to-noise ratio). Recently, the method has been also successfully applied on an orthotropic ribbed plate<sup>6</sup> and on bilayer plates<sup>7</sup>.

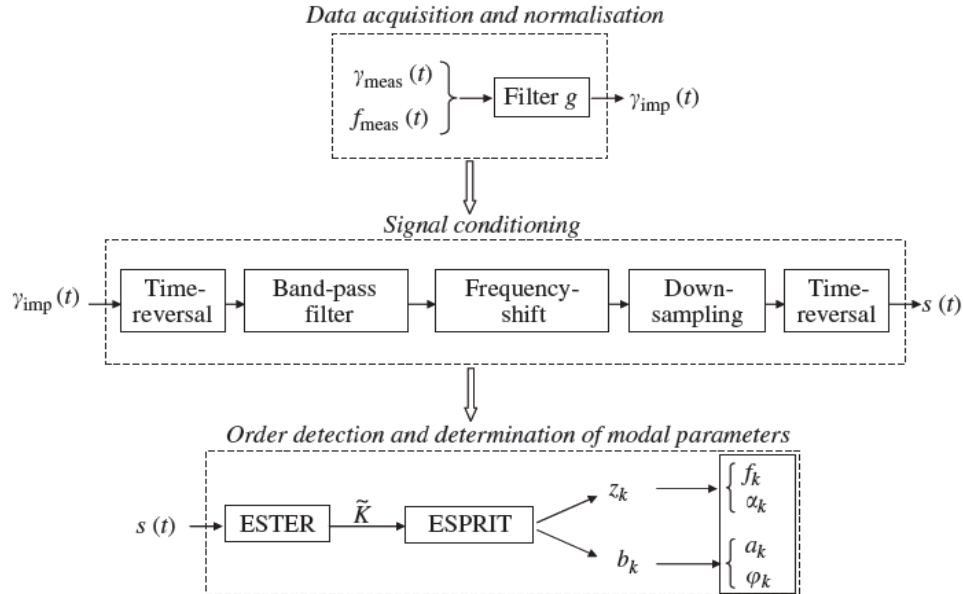


Fig.6 - Block diagram of the high-resolution modal analysis method (see Ege *et al.*<sup>1</sup> for details)

The equivalent loss factors of the SPS and SPA three-layers plates were accurately estimated using the method described above. The experimental protocol is similar to the previous section. The time signal  $s(t)$  analyzed with ESPRIT algorithm corresponds to an excitation made

in the vicinity of the accelerometer near one of the corner of the plate. A typical bank-filtering analysis of  $s(t)$  is given in Figure 7 for the SPS plate where results are plotted for one narrow subband of the mid-frequency domain with four identified modes. Equivalent loss factors have been estimated up to 2.6 kHz for the SPS plate (results are plotted on Figure 5) and up to 3 kHz for SPA plate (see results on Figure 8).

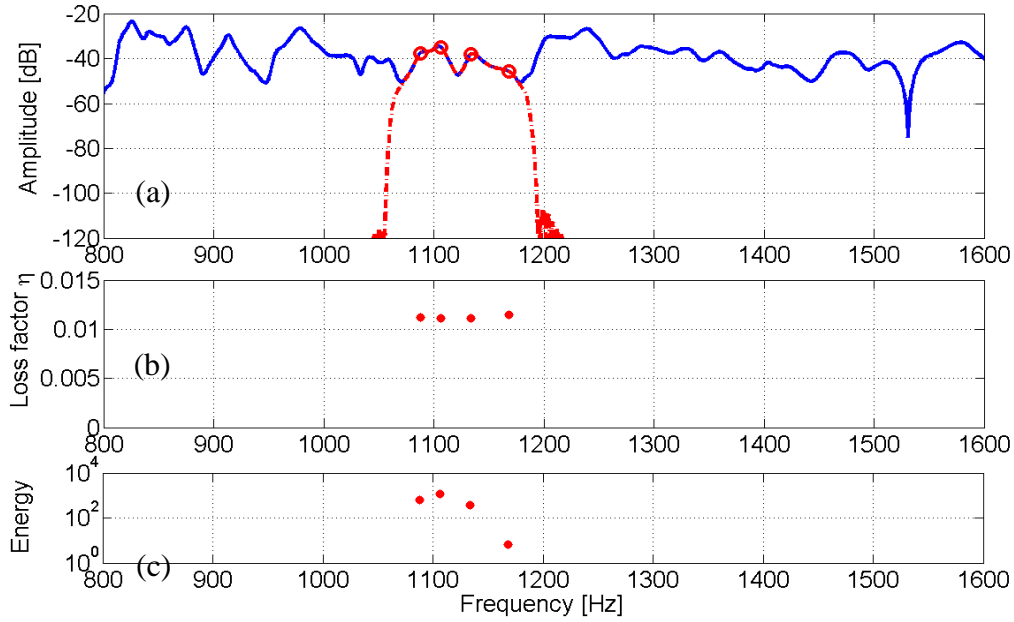


Fig.7. Typical bank-filtering analysis of an impulse response of the SPS plate between 1060 and 1180 Hz. (a) —: Fourier spectrum of the impulse response; —: amplitude response of a narrow-band filter.  $\bullet$  marks: estimated modal amplitudes and modal frequencies. (b)  $\bullet$  marks: measured loss factors  $\eta_k$  for the four real modes (the number of complex exponentials  $K=8$  ( $=2 \times 4$ ) is estimated with ESTER criterion). (c)  $\bullet$  marks: Energy of each components.

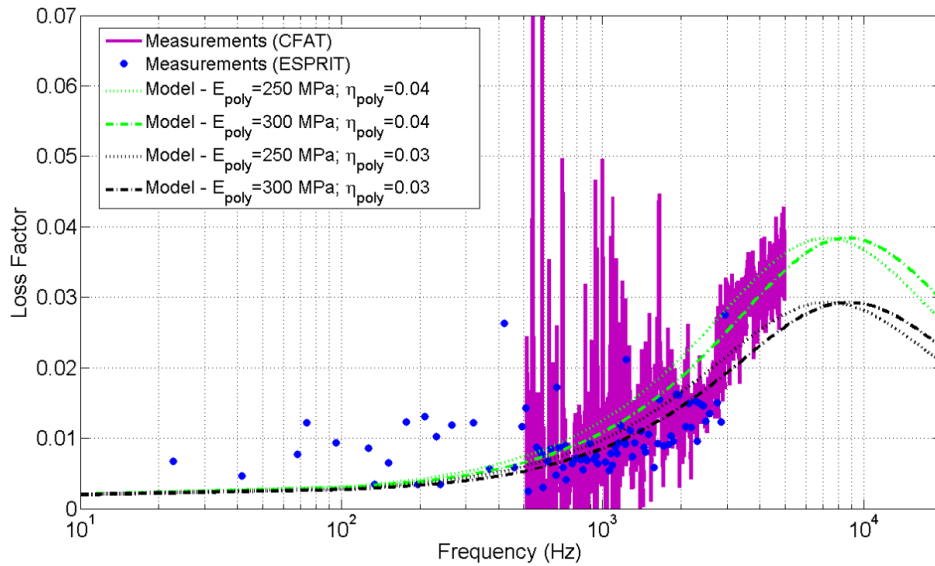


Fig. 8 –Equivalent loss factor  $\eta_{eq}$  – Steel/Polymer/Aluminum (SPA) plate – (same axis scale than Figure 5)



## 2.4 CFAT methodology in the mid and high-frequency domains – Equivalent complex Young's modulus

The FAT<sup>8</sup> (Force Analysis Technique) has been published about 20 years ago. The aim of this inverse approach is to recover excitation fields applied on structures from vibration measurements and an analytical form of the equation of motion. Typically, for thin homogeneous plates, the following equation is used at the angular frequency  $\omega$ :

$$D \nabla^4[w(x, y)] - \rho h \omega^2 w(x, y) = p(x, y) \quad (4)$$

where  $D = E(1 + j\eta)h^3/[12(1 - \nu^2)]$  is the complex rigidity of the plate and  $\rho h$  its mass per unit area (that are both known a priori),  $w(x, y)$  and  $p(x, y)$  are the displacement and load fields, respectively. The displacement  $w(x, y)$  is measured on a regular sampling mesh, and its fourth order spatial derivative is estimated using a corrected finite differences scheme CFAT<sup>9</sup>, allowing the estimation of the load field from other quantities.

The approach has been recently extended to application cases for which the structural parameters  $D$  and  $\rho h$  are unknown<sup>10,11</sup>. In these situations, the standard method is applied to areas of the structure that are *a priori* known to be excitation free. Equation (4) is thus used with  $p(x, y) = 0$ :

$$\frac{D}{\rho h} = \frac{\omega^2 w(x, y)}{\nabla^4[w(x, y)]} \quad (5)$$

The Young's modulus and loss factor are then obtained as follows:

$$E = \operatorname{Re}\left(\frac{D}{\rho h}\right) \frac{12\rho(1 - \nu^2)}{h^2}, \quad \eta = \frac{\operatorname{Im}\left(\frac{D}{\rho h}\right)}{\operatorname{Re}\left(\frac{D}{\rho h}\right)} \quad (6)$$

The mass per unit area  $\rho h$  and the thickness  $h$  are measured using static metrology systems (weighing machine, caliper...), the Poisson's ratio is arbitrarily adjusted from standard values, and the Young's modulus is obtained using Equation (6). When applied to homogeneous plates, the result is expected to be constant in the frequency range of validity of the CFAT method.

When applied to composite panels, the basic Equation (4) can still be used if the vibrational behavior of the plate is assumed to be governed by flexural waves. However, the structure being composed of several layers of materials with different moduli, the relationship between the rigidity  $D$  and Young's modulus is not valid anymore. A Young's modulus can still be estimated using Equation (6), but it correspond to the Young's modulus of an equivalent homogeneous plate of same thickness and mass per unit area, that would have observed the same vibrational displacement field at one given frequency. This Young's modulus, called the "equivalent Young's modulus", is not expected to be independent of the frequency anymore, as it was the case for homogeneous plates.

The two plates, SPS and SPA, presented in section 2.1 are freely suspended to a frame, and a shaker (driven by a white noise generator) is fixed at an arbitrary position on one edge. The velocity field of a part of the plate, free of any excitation, is measured using a scanning laser vibrometer. The scanning area is 27 x 39 cm, with a step of about 15 mm, that is to say a total of 513 measurement points. The CFAT, for both plates, was able to identify an equivalent Young's modulus on a frequency range from 500 Hz to 5 kHz. For SPS and SPA plates, results are

presented on Figures 4 and 9 for equivalent Young's moduli and on Figures 5 and 8 for equivalent loss factors.

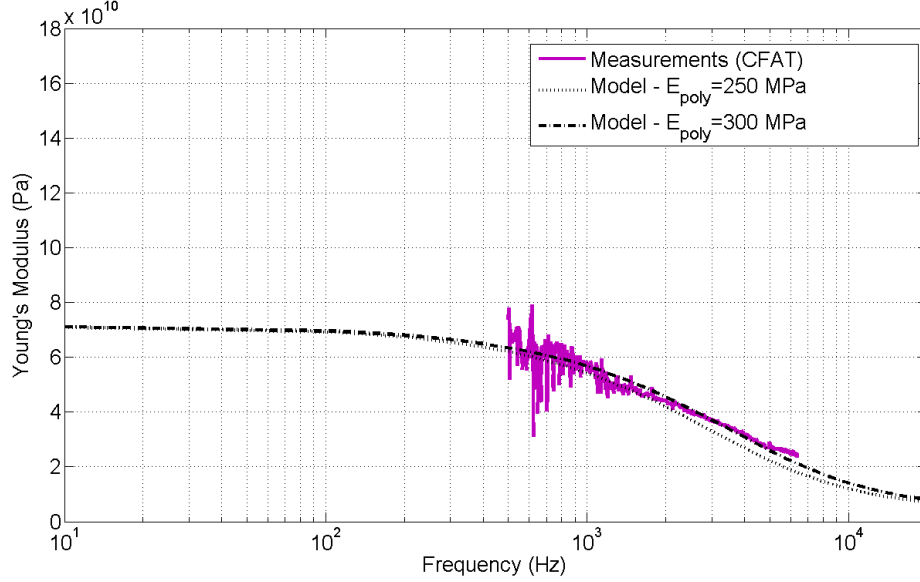


Fig. 9 –Equivalent Young's modulus  $E_{eq}$  – Steel/Polymer/Aluminum (SPA) plate – (same axis scale than Figure 4)

### 3 COMPARISON WITH AN EQUIVALENT SINGLE LAYER ANALYTICAL MODEL – POLYMER CORE MATERIAL CHARACTERISTICS IDENTIFICATION

#### 3.1 Equivalent single layer modeling

The analytical model developed by Guyader *et al.*<sup>12</sup> and implemented in the MOVISAND code<sup>13</sup>, calculates the equivalent complex Young's modulus  $\overline{E}_{eq} = E_{eq}(1 + j \eta_{eq})$  of a multi-layer viscoelastic plate (note that this equivalent modulus corresponds to the same modulus estimated with the CFAT method presented above for composite panels). The analytical method is based on the travelling wave approach applied to a simplified multi-layer model. In each layer bending, membrane and shear effects are considered. Continuity conditions on displacement and shear stresses at each layer interface are used to obtain the equations of motion of the multi-layered plate field expressed in the function of the first layer field<sup>12,13</sup>. Hence the method determines for a given frequency of calculation the equivalent single layer plate material (complex modulus) under Love-Kirchhoff thin plate theory in order of having same transverse displacement than the multilayer plate. The only parameters needed for the equivalent single layer modeling are thicknesses, densities and viscoelastic characteristics of each layer.

#### 3.2 Equivalent complex modulus of the three-layers – Polymer core complex modulus identification

For both SPS and SPA plates the frequency dependent equivalent Young's modulus and equivalent loss factors have been analytically predicted using the single layer plate modeling presented above. In our study, the major unknowns are the polymer core layer Young's modulus  $E_{poly}$  and loss factor  $\eta_{poly}$  (layer thickness has been measured, density has been deduced from weight measurements, and Poisson's ratio  $\nu$  is arbitrarily set to 0.34). For the steel and aluminum layers, standard values of the material characteristics have been taken and thicknesses have been measured. Thus, a fitting process has been conducted to identify the polymer core characteristics

needed to converge to the sandwich experimental estimations. Figures 4 and 9 display the equivalent Young's moduli obtained and Figures 5 and 8 the equivalent loss factors for SPS and SPA plates. For each figures the comparison is done between the different experimental estimations (CFAT, ESPRIT, modal analysis for SPS plate) and the analytical predictions with identified sets of parameters for the polymer core Young's modulus  $E_{poly}$  and loss factor  $\eta_{poly}$ .

The identification of these two quantities  $E_{poly}$  and  $\eta_{poly}$  is separated in two different steps. First, the fitting process consists in identifying first  $E_{poly}$  by converging to measured equivalent Young's modulus, in particular to CFAT estimations that covers several kHz. Figure 4 and Figure 9 concludes that this value is around  $E_{poly} = 250$  MPa (for frequencies between 100 Hz – 1 kHz) and tends to  $E_{poly} = 300$  MPa (higher, around 5 kHz). With  $E_{poly}$  estimated,  $\eta_{poly}$  is then fitted by comparing the predicted/measured equivalent loss factors (see Figures 5 and 8). This value has been identified around  $\eta_{poly} = 3 - 4$  %. It is interesting to note that the identified values are similar for the two systems as expected since the same polymer and processing routes are used for both symmetric and anti-symmetric plates.

With these identified polymer core characteristics, the predicted and experimental estimations of the multilayers equivalent parameters are in very good agreement. For the equivalent Young's modulus  $E_{eq}$  the tendency is particularly well predicted by the model. For SPS plate (Figure 4) the value is close to 150 GPa in the low-frequency domain and decreases to around 30 GPa at 5 kHz. For SPA plate (Figure 9) the trend is similar: the value is close to 70 GPa in low-frequencies and decreases to around 25 GPa at 5 kHz. This frequency dependent evolution of  $E_{eq}$  is well-known for metal-polymer-metal three-layer vibrating panels<sup>12,13</sup>: shear effects at layers interface increases with frequency, when wavelength shortens, decreasing thus the equivalent Young's modulus gradually.

For the equivalent loss factor  $\eta_{eq}$ , results are also very satisfying, even if the discrepancies are higher than for the real part estimation. Indeed, measured equivalent modal loss factor depends highly on modal radiation efficiency that can vary a lot from one mode to the other in the low-frequency range in particular. This contribution is not predicted by the analytical model that doesn't take into account radiation losses, estimating only the structural loss factor (related to the imaginary part of the complex modulus). Nevertheless the experimental loss factor frequency evolution match well the equivalent single layer modeling predictions for both SPS (Figure 5) and SPA (Figure 8) plates. In the low frequency part, damping is small and close to the metal losses (around 0.5%); then it regularly increases with rising frequency and attains very high values (around 10 times more) at 5 kHz for last CFAT estimations: that means  $\eta_{eq}$  around 5 % for SPS plate and 4 % for SPA plate. Here again the increasing of shearing of the dissipative polymer core layer is responsible for this large increase of damping. Such results shows all the benefits of using sandwich three-layer for vibroacoustics applications in terms of high-damping properties for given frequency domains. With such experimental and analytical approaches presented in this paper, optimization of multi-layer plates with optimized damping properties for given frequency domains may be easily performed.

### 3.3 Comparison of the estimated Young's modulus of the polymer with DMA measurements

With the aim of evaluating the validity of our inverse method to identify the polymer core properties, the low frequency complex modulus of the polymer alone was measured using

Dynamic Mechanical Analysis. In details, the polymer rectangular samples were loaded in tensile mode and the modulus was evaluated for three frequencies (1, 5 and 25 Hz) over a wide range of temperature encompassing room temperature (240 K – 380 K). The real contribution of the complex modulus, corresponding to the Young's modulus, is displayed in Figure 10: for a given frequency, the modulus is seen to decrease as the temperature increase. Similarly, for a given temperature, the modulus is seen to increase as the loading frequency increases, consequence of the time-temperature equivalence.

Based on the aforementioned principle, Blachot *et al.*<sup>14</sup> developed a simple method to build up the polymer mastercurve based on three isochronal measurements profiles. The method was implemented in a *Matlab* routine and the prediction of the polymer performance can be obtained for a range of frequencies that is greater than the range experimentally achievable. This is evidenced in Figure 10, where the predicted modulus for frequencies ranging from 100 Hz to 100 kHz are displayed.

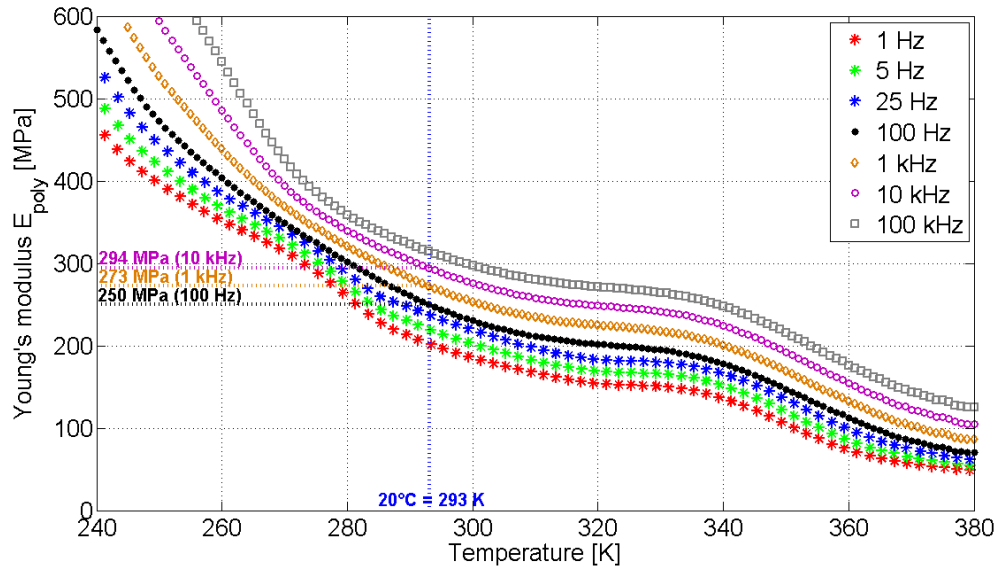


Fig. 10 –Young's modulus of the polymer core for different temperatures and frequencies obtained through DMA measurements (1, 5 and 25 Hz) and extrapolations (100 Hz, 1 kHz, 10 kHz and 100 kHz).

The DMA measurements and extrapolations can then be used to read the modulus at room temperature (20° C). Focusing on the high frequencies values, the polymer modulus  $E_{poly}$  is found to be about 250 MPa at 100 Hz, 273 MPa at 1 kHz, and 294 MPa at 10 kHz (see Figure 10). It is worth noticing that these predictions accurately match the values identified based on the vibratory approach depicted in the previous section, demonstrating the validity of the inverse methodology developed. Same conclusions can be drawn on the imaginary part (not presented here).

#### 4 CONCLUSIONS & PERSPECTIVES

This paper is focused on the vibrational behavior of three-layer (metal-polymer-metal) composites plates. Equivalent Young's moduli and equivalent loss factors of two different sandwich systems are estimated in broad-band frequency range using different experimental methods. The results are in very good agreement with an equivalent single layer analytical modeling based on wave propagation analysis. The comparison with this theoretical approach

allows identifying the frequency dependent complex modulus of the polymer core layer through inverse resolution that matches DMA measurements/predictions performed on the polymer material alone.

There are several perspectives and applications of this work. With the approach presented in this paper, optimization of multi-layer plates for vibroacoustics applications, with optimized damping properties for given frequency domains, may be easily performed. In order to improve the comparison of experimental results with analytical estimations, the precise knowledge of the frequency evolution of the complex Young's modulus of the polymer core is crucial.

## 5 ACKNOWLEDGEMENTS

This work was carried out in the framework of the LabEx CeLyA (Centre Lyonnais d'Acoustique, ANR-10-LABX-60) and the VIVARIUM project (BQR 2014-2015 funded by INSA-Lyon). The authors would like to thank master's student Eddy Fasana for his help during measurements.

## 6 REFERENCES

1. K. Ege, X. Boutillon, and B. David, "High-resolution modal analysis", *Journal of Sound and Vibration*, **325**(4-5), 852–869, (2009)
2. R. Roy and T. Kailath, "Esprit - estimation of signal parameters via rotational invariance techniques", *IEEE Transactions on Acoustics Speech and Signal Processing*, **37**(7), 984-995, (1989)
3. D. J. Ewins, *Modal testing*. Research studies press, (1984)
4. R. Badeau, B. David and G. Richard, "A new perturbation analysis for signal enumeration in rotational invariance techniques", *IEEE Transactions on Signal Processing*, **54**(2), 450-458, (2006)
5. J. Laroche, "The use of the matrix pencil method for the spectrum analysis of musical signals", *Journal of the Acoustical Society of America*, **94**(4), 1958-1965, (1993)
6. K. Ege, X. Boutillon and M. Rébillat, "Vibroacoustics of the piano soundboard: (Non)linearity and modal properties in the low- and mid-frequency ranges", *Journal of Sound and Vibration*, **332**(5), 1288-1305, (2013)
7. K. Ege, T. Boncompagne, B. Laulagnet and J.-L. Guyader, "Experimental estimations of viscoelastic properties of multilayer damped plates in broad-band frequency range", *Proceedings of Internoise 2012*, New York, USA, (2012)
8. C. Pézerat and J.-L. Guyader, "Force analysis technique: Reconstruction of force distribution on plates", *Acustica united with Acta Acustica*, **86**, 322-332, (2000)
9. Q. Leclère and C. Pézerat, "Vibration source identification using corrected finite difference schemes", *Journal of Sound and Vibration*, **331**(6), 1366-1377, (2012)
10. F. Ablitzer, C. Pézerat, J.-M. Génevaux and J. Bégué, "Identification of stiffness and damping properties of plates by using the local equation of motion", *Journal of Sound and Vibration*, **333**(9), 2454-2468, (2014)
11. Q. Leclère, F. Ablitzer and C. Pézerat, "Practical implementation of the corrected force analysis technique to identify the structural parameter and load distributions", *Journal of Sound and Vibration*, In Press, Corrected Proof, Available online 14 May 2015, [doi:10.1016/j.jsv.2015.04.025](https://doi.org/10.1016/j.jsv.2015.04.025)
12. J.-L. Guyader and C. Lesueur, "Acoustic transmission through orthotropic multilayered plates, Part 1: plate vibration modes", *Journal of Sound and Vibration*, **58**(1), 51-68, (1978)
13. J.-L. Guyader and C. Cacciolati, "Viscoelastic properties of single layer plate material equivalent to multi-layer composites plates", *Proceedings of Inter-Noise 2007*, Istanbul, Turkey, (2007)
14. J.-F. Blachot, L. Chazeau, and J.-Y. Cavaille, "Rheological behavior of cellulose/monohydrate of N-methylmorpholine N-oxide solutions. Part 2. Glass transition domain", *Polymer*, **43**(3), 881-889, (2002)